PAPER

Effects of Bragg Scattering on Ultra-Wideband Signal Transmission from Periodic Surfaces

Hiroaki TSUCHIYA[†a)], Navarat LERTSIRISOPON[†], *Student Members*, Jun-ichi TAKADA[†], *and* Takehiko KOBAYASHI[††], *Members*

SUMMARY In this paper, the effects of Bragg scattering on ultra-wideband (UWB) signal transmission from periodic surfaces are reported. First, the frequency dispersive property of Bragg scattering is theoretically and experimentally confirmed. Next, the transfer function of both specular path and Bragg scattering are extracted. Then direct sequence UWB (DS-UWB) transmission simulations are conducted by using a raised cosine pulse that occupied 3.1 to 10.6 GHz and a Gaussian pulse that occupied 8.75 to 9.25 GHz. Finally, the effects of Bragg scattering on UWB systems are discussed.
key words: *Bragg scattering, ultra-wideband, UWB transmission, propagation*

1. Introduction

In indoor and outdoor propagation environments, nonspecular scattering is often not negligible. While Bragg scattering [1]–[3] have been discussed with regard to river or sea surfaces [4], it may also be significant for periodic structures such as brick walls, metallic shutters and window blinds. In particular, its frequency dispersive property [5] may influence the transmission performance of ultra-wideband (UWB) systems [6]–[8]. Our previous works [9]–[11] presented the theoretical analysis and also confirmed the existence of Bragg scattering by doing experiments using metallic window blinds as periodic structures. In this paper, we focus on the effects of Bragg scattering on direct sequence UWB (DS-UWB) [12]–[14] signal transmission from periodic surfaces, and investigate how Bragg scattering deteriorate UWB waveforms and degrade UWB transmission performances by conducting transmission simulations.

2. Bragg Scattering Experiment

2.1 Definition of Bragg Scattering

Bragg's law [1] defines a reflection or diffraction relationship between the wavelength of an incoming ray path and the period of the periodic structure. Figure 1 illustrates the Bragg scattering when rays 1 and 2 are reflected from peak points 1 and 2, respectively. When the path length difference Δl of the two rays satisfies Eq. (1), Bragg scattering exists, and its scattering angle follows Eq. (2)

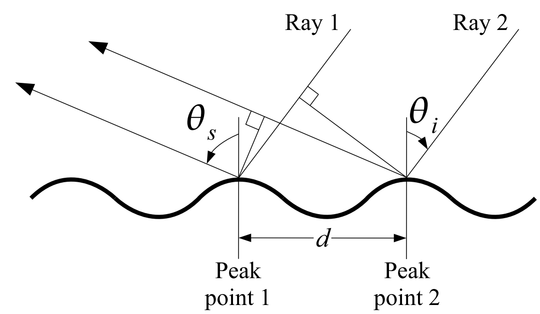

Fig. 1 Bragg scattering illustration.

$$\Delta l = d \sin\theta_i - d \sin\theta_s = n\lambda \tag{1}$$

$$\theta_s = \arcsin\left(\sin\theta_i - \frac{n\lambda}{d}\right) \tag{2}$$

where

- n: the order of reflection ($n = \pm1, \pm2, \cdots$),
- λ: the wavelength of the incident ray,
- d: the period of periodic structure,
- θ_i: the incident angle,
- θ_s: the reflection (scattering) angle.

The case that $n = 0$ in Eq. (1) corresponds to specular reflection.

2.2 Experiment Setup

Figure 2 shows the measurement setup. The measurements were performed with a vector network analyzer (VNA) to determine the complex radio channel transfer function $H(f) = S_{21}(f)$. Selected parameters are listed in Table 1. The transmitting antenna was mounted on a fixed pole and the receiving antenna was vertically scanned to measure the direction of arrival (θ_s). We used metallic window blinds (case A) and a metallic white board (case B) to compare the difference between the periodic and flat surfaces. The details are shown in Fig. 3.

2.3 Theoretical Analysis and Experiment Results

From the experiment setup, Tx and Rx positions bound the

Manuscript received March 30, 2007.
Manuscript revised August 6, 2007.
[†]The authors are with the Department of International Development Engineering, Graduate School of Science and Engineering, Tokyo Institute of Technology, Tokyo, 152-8550 Japan.
[††]The author is with Tokyo Denki University, Tokyo, 101-8457 Japan.
a) E-mail: tutiya@ap.ide.titech.ac.jp
DOI: 10.1093/ietcom/e91–b.2.536

possible range of θ_i and θ_s to $0° \le \theta_i \le 65°$ and $-47° \le \theta_s \le 57°$, respectively. Its theoretical analysis of Bragg scattering based on Eq. (2) and blind spacing (the period of periodic structure d) of 2.1 cm is also shown in Fig. 4 on which Bragg scattering was theoretically confirmed.

For case A, since Bragg scattering has frequency dispersive properties, we show the frequency-angle power spectrum (Fig. 5) and frequency-delay spectrogram (Fig. 6) separately. Figures 5 and 6 were computed by using beam-

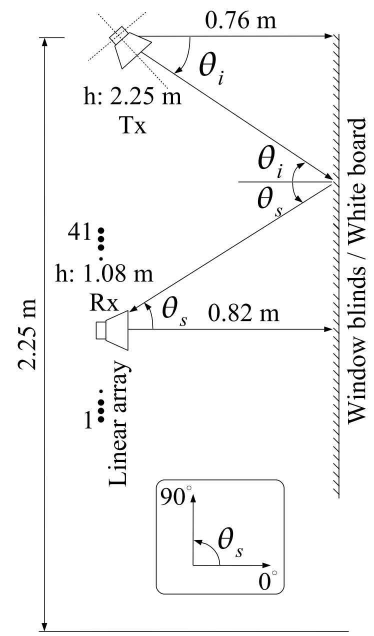

Fig. 2 Experiment setup.

Table 1 Specifications of the experiment.

Bandwidth	3.1 to 10.6 GHz
Frequency sweeping points	751
Spatial sampling in the Rx position	41 points in vertical linear array whose element spacing is 1 cm
Height of Tx and Rx	Tx: 2.25 m, Rx: 0.88 to 1.28 m
Type of antennas	Double-ridged guide horn
Polarization	Vertical-Vertical
Calibration	Function of VNA
SNR at receiver	about 50 dB

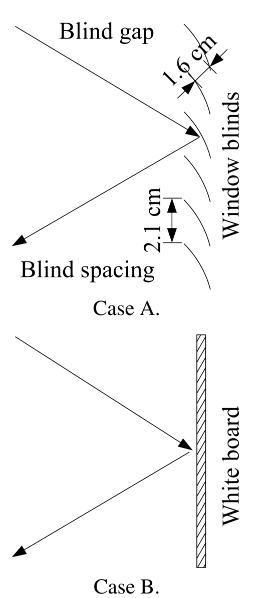

Fig. 3 Target objects.

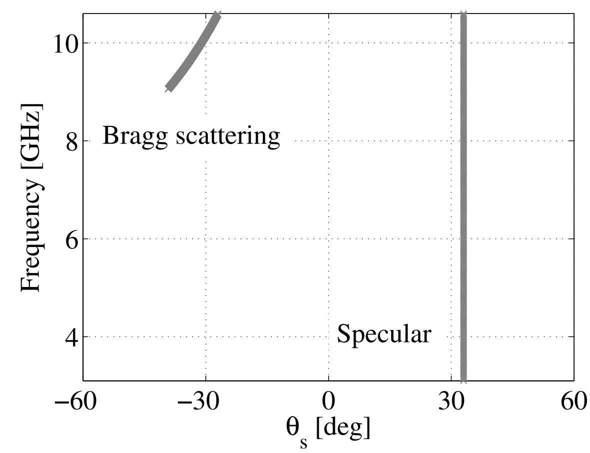

Fig. 4 Bragg scattering theoretical analysis of case A.

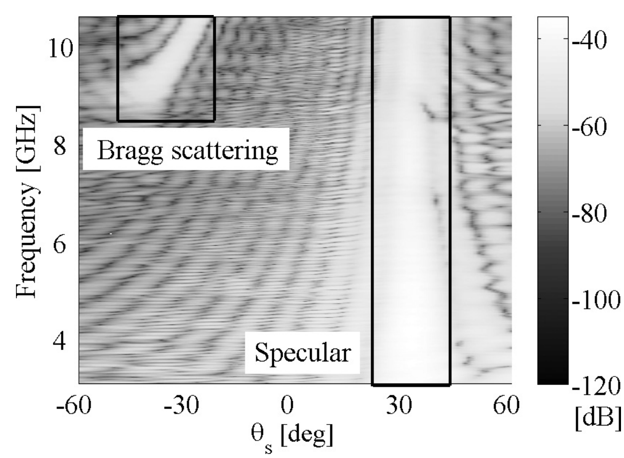

Fig. 5 Frequency-angle power spectrum of case A.

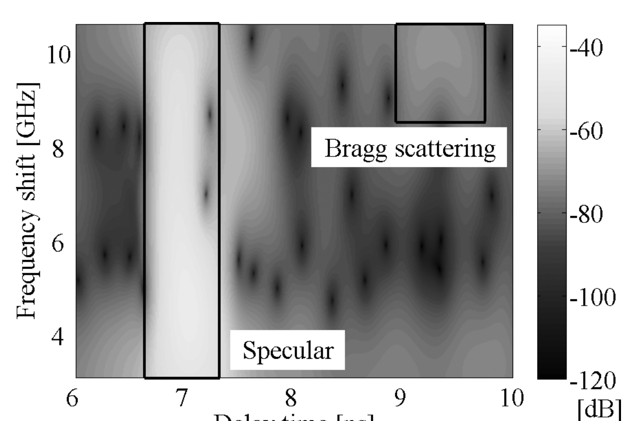

Fig. 6 Frequency-delay spectrogram of case A.

forming [15]–[17] and short period inverse Fourier transform respectively. A hanning window with 751 points was shifted across each frequency sweeping point for the inverse Fourier transform to detect Bragg scattering both in time and frequency domain. Bragg scattering and the specular reflection can be found as marked areas in these figures. Comparing Figs. 4 and 5, it can be said that the theoretical analysis result agrees with the experiment, and Bragg scattering with a wide angular spread appeared at the high frequency part in this experiment setup. Moreover, it is shown in Fig. 6 that Bragg scattering appeared with a long delay spread on a different delay time compared to the specular path.

For case B, no Bragg scattering was found since the reflecting object (white board) has a flat surface. Its specular reflection was found at the same position as case A.

3. Specular Paths and Bragg Scattering

According to Figs. 5 and 6, the specular path and Bragg scattering can be separated both in angular and time domain, so it is possible to detect the specular path by using a matched filter both in angular and time domain. The path gain values for both cases are shown in Table 2.

Figure 7 shows the transfer function of specular path for both cases. Since the materials of the objects for cases A and B are different, they have different losses. The loss of case A is approximately 2 dB greater than case B, and it can be confirmed at frequencies lower than 8.43 GHz. From 8.43 to 9.48 GHz, a significant dip can be observed at specifically 8.98 GHz due to the influence of Bragg scattering. This range falls in the frequency range of Bragg scattering shown in Fig. 5, and means that the specular path are affected by Bragg scattering. For the part greater than 9.48 GHz, there is almost no effect from Bragg scattering, but the penetration loss for case A should be considered because the half wavelength ($\lambda/2$) at these frequencies are smaller than the blind gap (about 1.6 cm), and therefore the specular path at these frequencies can go through the blind gap.

For Bragg scattering, it cannot be detected as one path. The frequency dispersion of Bragg scattering resulted in a relatively long delay spread and a wide angular spread as listed in Table 2, and no significant peak can be observed. One transfer function (at 9.5 ns, −36°) of Bragg scattering for both cases are shown in Fig. 8. Note that although there is no Bragg scattering for case B, we show the transfer function of case B with the similar angular and delay information as in case A in order to make a comparison. As we can see, there is almost no difference up to 8.43 GHz between cases A and B, therefore no additional signal can be received at the receiver due to Bragg scattering. But for frequencies from 8.43 to 9.48 GHz (maximum at 8.98 GHz, this value follows the frequency corresponding to $\theta_s = -36°$ as shown in Fig. 5), Bragg scattering for case A may deteriorate UWB waveforms with its high gain components and degrade UWB transmission performances.

Table 2 Results of cases A and B.

	case A		case B	
	Specular	Bragg scattering	Specular	Bragg scattering
θ_s [deg]	33	−50 to −25	33	-
Delay [ns]	7.0	9.0 to 9.8	7.0	-
Frequency range [GHz]	whole	above 8.5	whole	-
Gain [dB]*	−42.59	−68.23(mean)	−40.26	-

(* Tx and Rx antenna gains are included.)

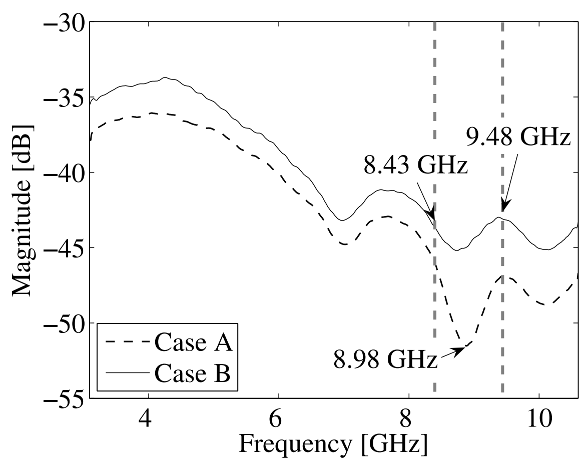

Fig. 7 Transfer function of specular paths (at 7.0 ns, 33°).

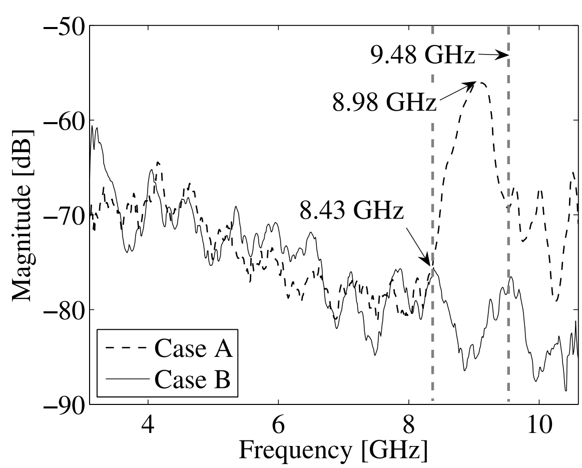

Fig. 8 Transfer function of Bragg scattering (at 9.5 ns, −36°).

4. Transmission Simulation

In order to know how Bragg scattering may deteriorate UWB waveforms and degrade UWB transmission performances, transmission simulations were conducted by using the transfer functions shown in Sect. 3 and two signal pulses with equations shown in Eqs. (3) and (4). One consideration in choosing the signal pulses is that it must have a clear peak in the time domain so that we can clearly compare the received and transmitted pulses. Moreover, since Bragg scattering may have a bad influence on the high frequency part of the specular path for case A, it is better to use a limited band signal pulse whose frequency range is wider than the 8.43 to 9.48 GHz range and another signal pulse within the 8.43 to 9.48 GHz range to see the effect of both on Bragg scattering. Due to these issues, a raised cosine pulse (RCP) that occupied the whole UWB range from 3.1 to 10.6 GHz, and a Gaussian pulse (GP) that occupied the position with Bragg scattering centered at 9 GHz with 500 MHz bandwidth were used. For RCP, instead of the low (3.1 to 4.9 GHz) and high (6.2 to 9.7 GHz) bands as proposed in [12], the full band signal pulse from 3.1 to 10.6 GHz was used for convenience. Both RCP and GP transmit through the channels of specular path and Bragg scattering. The RCP is given as follows [18]:

$$x(t) = \frac{\sin(\pi t/t_d)}{\pi t/t_d} \cdot \frac{\cos(\alpha \pi t/t_d)}{1-(2\alpha t/t_d)^2} \tag{3}$$

where

- $f_c = 6.85$ GHz: the center frequency,
- $t_d = 1/7.5$ ns: the duration of the pulse,
- $\alpha = 0$: the roll-off factor,

and, the GP is given as follows:

$$x(t) = \exp(2t/t_d)^2 \cos(2\pi f_c t) \tag{4}$$

where

- $f_c = 9$ GHz: the center frequency,
- $t_d = 1/0.5$ ns: the duration of the pulse.

Figures 9 and 10 show the transmitted signal of the RCP and GP in time and frequency domains respectively. The received signal $s(t)$ is constructed as follows:

$$S(f) = X(f)H_{\tau,\theta_s}(f) \tag{5}$$

$$s(t) = \mathcal{F}^{-1}\Big[S(f)\Big] \tag{6}$$

where $X(f)$ is the Fourier transform of $x(t)$, $H_{\tau,\theta_s}(f)$ is the transfer function with delay and angular information including both Tx and Rx antenna gains, and $\mathcal{F}^{-1}[\cdot]$ is the inverse Fourier transform.

According to the IEEE 802.15 Task Group 3a [6], DS-UWB is one of the standards considered for UWB high-speed wireless personal area network (WPAN) [19] systems. It is based on the direct sequence spread spectrum (DSSS) [20] technology where a rake receiver is useful for collecting scattered signal energy over multipaths. The multipaths can be collected by using a rake receiver, and signal symbols are detected using correlative detection by comparing received waveforms with transmitted waveforms. In order to evaluate numerically the received waveform deterioration due to Bragg scattering, we show the correlation value between received waveforms and transmitted waveforms (shown in Figs. 9(a) and 10(a)) both for RCP and GP in Table 3. However, to know how Bragg scattering may degrade UWB transmission performances, not only waveform deteriorations should be considered, but the gain and delay spread of received signals are also important because

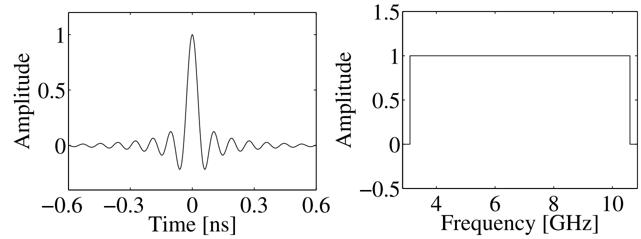

(a) Time domain. (b) Frequency domain.

Fig. 9 Transmission signal (RCP: 7.5 GHz bandwidth) in time and frequency domain.

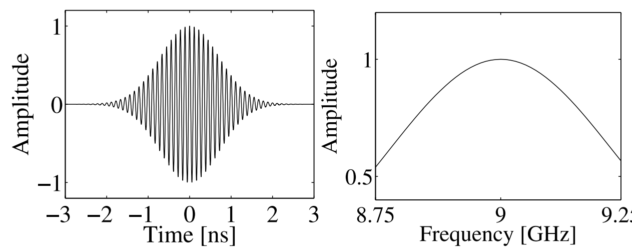

(a) Time domain. (b) Frequency domain.

Fig. 10 Transmission signal (GP: 500 MHz bandwidth) in time and frequency domain.

Table 3 Correlation between transmitted and received waveforms.

	3.1 to 10.6 GHz (RCP)		8.75 to 9.25 GHz (GP)	
	Specular	Bragg scattering	Specular	Bragg scattering
Correlation**	0.78	0.26	0.94	0.97

(** Tx and Rx antenna distortions are included.)

the receiver need these information to collect multipaths and DS-UWB system performance may suffer from long delay spread and low gain pluses. Note that the information of delay and gain are shown in Table 2. In the following figure explanations, the received waveforms by transmitting RCP and GP pulses to the transfer functions shown in Sect. 3 are discussed.

Figure 11 shows the RCP received waveforms of specular path for both cases, both waveforms were affected by the antenna characteristics. As we can see, there is only a slight influence that can be observed from Bragg scattering for case A. Because the specular path was only affected by Bragg scattering at high frequencies, the signal can be detected due to its high correlation value with the transmitted waveform. However, if the size of the periodic rough surface is large (ex. 4.0 cm), not only one Bragg scattering can be confirmed, but another Bragg scattering can also exist at lower frequencies and affect the specular path as will be discussed in Sect. 5.

Figure 12 shows the RCP received waveform of Bragg scattering for case A. Note that this paper shows the received waveform of Bragg scattering separately from the specular path in the time domain because their transfer functions are different in the angular domain, and the time resolution both for RCP and GP are enough to separate the specular path and

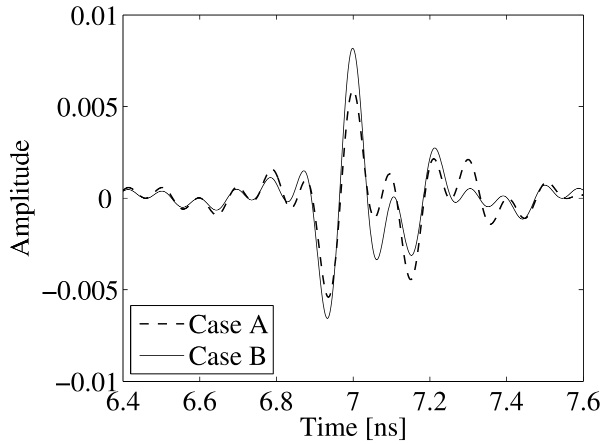

Fig. 11 Received waveforms (RCP: 7.5 GHz bandwidth) using transfer function of specular path for both cases.

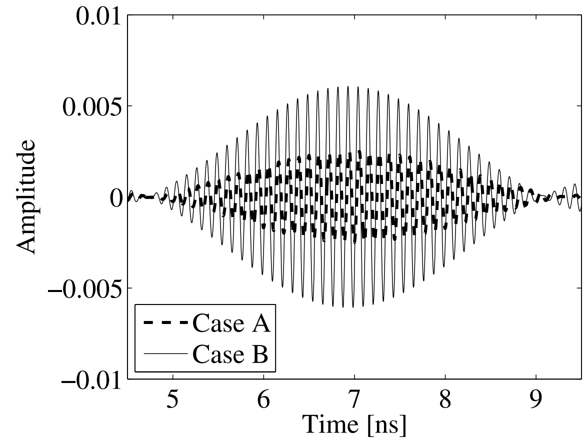

Fig. 13 Received waveforms (GP: 500 MHz bandwidth) using transfer function of specular path for both cases.

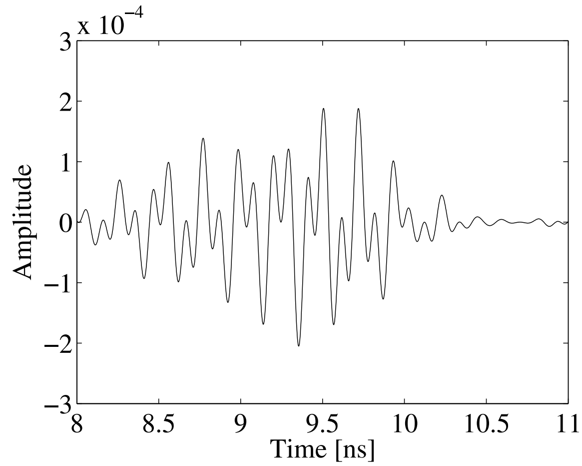

Fig. 12 Received waveform (RCP: 7.5 GHz bandwidth) using transfer function of Bragg scattering for case A.

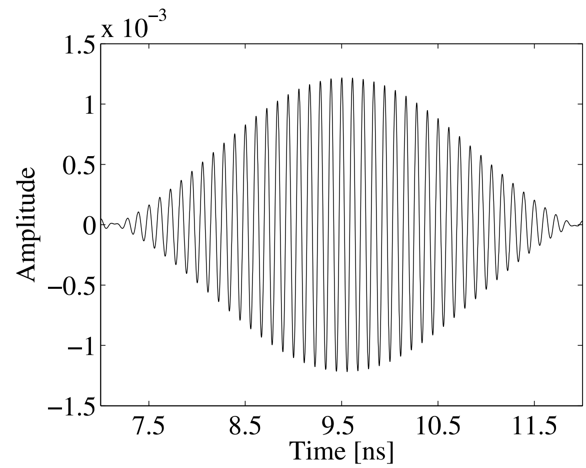

Fig. 14 Received waveform (GP: 500 MHz bandwidth) using transfer function of Bragg scattering for case A.

Bragg scattering. As we can see, it is quite different from the original waveform shown in Fig. 9(a). It has a low correlation value with the transmitted waveform because only the high frequency component is received by the receiver. Its long delay spread may destroy path detection and affect the system.

Figure 13 shows the GP received waveforms of specular path for both cases, both waveforms are similar to the original waveforms shown in Fig. 10(a) but the received power in case A is lower than in case B, because power of case A was reduced by Bragg scattering. In addition, the antenna characteristics cannot be observed clearly compared to the RCP received waveforms.

Figure 14 shows the GP received waveform of Bragg scattering. It has a high correlation value with the transmitted waveform, so that it is different from the the fullband case (Fig. 12), but the delay spread should also be considered in the system performance.

5. Variation of the Period of Periodic Structure

Since Bragg scattering also depends on the period of periodic structure d, the question is how Bragg scattering may deteriorate UWB waveforms and degrade UWB transmission performances by changing the period of periodic structure d. We use the theoretical analysis instead of using experiments because it is too difficult to find spacing-changeable window blinds. The theoretical analysis based on Eq. (2) was simulated by changing the value d from 3.0 to 6.0 cm, and its results are shown in Fig. 15. Note that Bragg scattering can only be observed for d larger than 1.9 cm, as this relates to the frequency range from 3.1 to 10.6 GHz and the incident angle setup. From Fig. 15, we can see that the number of Bragg scattering increased when the periodic distance gets bigger. This increased number of Bragg scattering will affect the specular path more and will severely degrade UWB transmission performances.

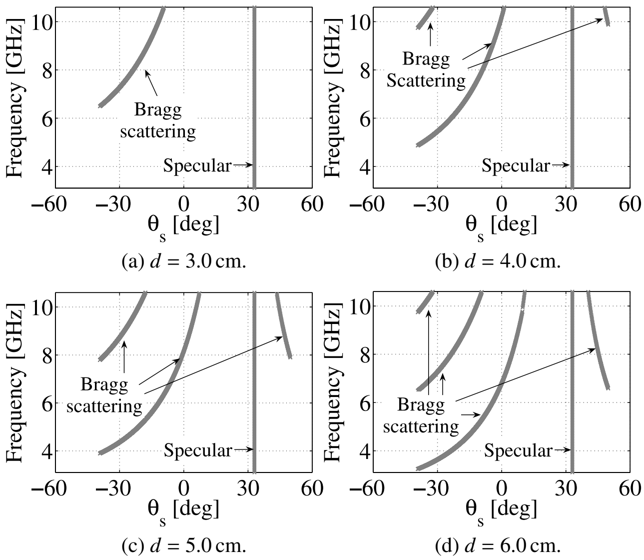

Fig. 15 Bragg scattering theoretical analysis for the different period of periodic structure *d*.

6. Conclusion

In this paper, the effects of Bragg scattering on UWB signal transmission from periodic surfaces were reported. The frequency dispersive property of Bragg scattering was theoretically and experimentally confirmed and the effects of Bragg scattering on DS-UWB transmissions were discussed based on simulation results. For specular path, only the waveform of full band signal pulses may be affected when some parts of the waveform's spectrum are deteriorated by Bragg scattering which depends on the period of the periodic rough surface, and the waveform of limited band signal pulses may not be deteriorated by Bragg scattering, although its gain may be reduced. For Bragg scattering components, only the waveform of full band signal pulses may be affected by Bragg scattering, and the waveform of limited band signal pulse may not be deteriorated. But the delay spread for both full and limited band signal pulses should be considered. For future work, we plan to consider about changing the angle of blind and polarization, so that the variable gain due to different angle of blind may be observed.

Acknowledgment

The authors would like to thank Mr. Kriangsak Sivasondhivat and Mr. Gilbert Siy Ching from Tokyo Institute of Technology for the helpful discussions and proofreading of this paper.

References

[1] M. Born and E. Wolf, Principles of Optics 7th (expanded) ed., pp.705–708, Cambridge University Press, 2001.
[2] M.I. Skolnik, Radar handbook 2nd ed., pp.1329–1331, McGraw-hill, 1990.
[3] M.W. Long, Radar reflectivity of land and sea, p.84, Artech House, 1991.
[4] W.J. Plant, W.C. Keller, K. Hayes, and R. Contreras, "Measurement of river surface currents using rough surface scattering," 2005 IEEE Antennas and Propagation Society International Symposium, vol.1A, pp.380–383, July 2005.
[5] R. Vaughan and J.B. Andersen, Channel, propagation and antennas for mobile communications, The Institute of Electrical Engineers, pp.209–210, 2003.
[6] http://www.ieee802.org/15/pub/TG3a.html
[7] R. Kohno, "Overview of UWB systems trends of R & D and regulation," 2003 Microwave Workshop & Exhibition (MWE2003) Digest, Nov. 2003.
[8] T. Kobayashi, F. Ohkubo, N. Takahashi, M. Yoshikawa, T. Miyamoto, H. Zhang, J. Takada, and K. Araki, "Overview and trends of UWB (ultra wideband) propagation studies," IEICE Technical Report, WBS2003-1, May 2003.
[9] N. Lertsirisopon, H. Tsuchiya, M. Ghoraishi, J. Takada, and T. Kobayashi, "Investigation of the Bragg scattering of UWB signal from the window blind: (1) Theoretical investigation," Proc. IEICE Gen. Conf.'06, B-1-2, March 2006.
[10] H. Tsuchiya, N. Lertsirisopon, M. Ghoraishi, J. Takada, and T. Kobayashi, "Investigation of the Bragg scattering of UWB signal from the window blind: (2) Experimental investigation," Proc. IEICE Gen. Conf.'06, B-1-3, March 2006.
[11] H. Tsuchiya, N. Lertsirisopon, M. Ghoraishi, J. Takada, and T. Kobayashi, "Influence of Bragg scattering on UWB signal reflection from a periodic surface," Proc. Society Conf. IEICE'06, AS-2-3, March 2006.
[12] M. Welborn, "DS-UWB proposal update," IEEE 802.15-05-274-00, May 2005.
[13] J.R. Foerster, "The performance of a direct-sequence spread ultra-wideband system in the presence of multipath, narrowband interference, and multiuser interference," Proc. IEEE Conf. on UWBST 2002, May 2002.
[14] M.M. Laughlin, M. Welborn, and R. Kohno, "Summary presentation of the Xtreme spectrum proposal," IEEE P802.15-03-334r5, Sept. 2003.
[15] H. Krim and M. Viberg, "Two decades of array signal processing research," IEEE Signal Process. Mag., July 1996.
[16] B.D. Van Veen and K.M. Buckley, "Beamforming: A versatile approach to spatial filtering," IEEE ASSP Magazine, April 1998.
[17] D.H. Johnson and D.E. Dudgeon, Array signal processing concepts and techniques, pp.111–190, Prentice Hill PTR, 1993.
[18] T.S. Rappaport, Wireless communications principles and practice, pp.227–283, Prentice Hall PTR, 1996.
[19] http://grouper.ieee.org/groups/802/15/
[20] M.B. Pursley, "Direct-sequence spread-spectrum communications for multipath channels," IEEE Trans. Microw. Theory Tech., vol.50, no.3, pp.653–661, March 2002.

Hiroaki Tsuchiya received the B.E. degree from Tokyo University of Agriculture and Technology, Tokyo, Japan, in 2003, and M.E. degree from Tokyo Institute of Technology, Tokyo, Japan, in 2005. At present, he is studying towards a Ph.D. degree at Tokyo Institute of Technology, Tokyo, Japan. His research interests focus on the wireless propagation channel characterization and modeling of ultra wideband radio. He received the IEICE Technical Group of Wideband System student paper award in 2006. He is a student member of IEEE.

Navarat Lertsirisopon received the B.E. degree from Sirindhorn International Institute of Technology, Thammasat University, Bangkok, Thailand, in 2002, and M.E. degree from Tokyo Institute of Technology, Tokyo, Japan, in 2006. Presently, she is studying towards the Ph.D. degree at Tokyo Institute of Technology, Tokyo, Japan. Her current research interest is propagation prediction modeling in wireless communication systems.

Jun-ichi Takada received the B.E. and D.E. degrees from Tokyo Institute of Technology, Japan, in 1987 and 1992, respectively. From 1992 to 1994, he has been a Research Associate at Chiba University, Chiba, Japan. From 1994 to 2006, he has been an Associate Professor at Tokyo Institute of Technology, Tokyo, Japan. Since 2006, he has been a Professor at Tokyo Institute of Technology. His current research interests are wireless propagation and channel modeling, antennas and antenna systems for wireless applications, and cognitive radio technology. He is a member of IEEE, ACES, and ECTI Association Thailand.

Takehiko Kobayashi received the B.E., M.E., and Ph.D. degrees in electrical engineering from the University of Tokyo, Tokyo, Japan, in 1978, 1980, and 1983. In 1983, he joined Nippon Telegraph and Telephone, where he was engaged in research on various wireless communication systems. In 1986, he was a guest scientist with the National Bureau of Standards (now the National Insitute of Standards and Technology), Boulder, CO, U.S.A. From 1998 to 2001, he was with YRP Key Tech Labs, where he focused on fourth-generation mobile communication systems. He is currently a Professor with the Department of Information and Communication Engineering, Tokyo Denki University, Tokyo, Japan. He received the IEICE Best Paper Awards in 2001 and 2002 and the Telecom System Awards from the Telecommunications Advancement Foundation in 2003 and 2005. His current research interests include UWB wireless systems, mobile communication channel characterization, and teletraffic evaluation of mobile communication networks. Dr. Kobayashi is a member of IEEE.